$Ag_{1-x}Na_xNbO_3$ (ANN) solid solutions: from disordered antiferroelectric $AgNbO_3$ to normal antiferroelectric $NaNbO_3$

1999 J. Phys.: Condens. Matter 11 8933

(http://iopscience.iop.org/0953-8984/11/45/316)

J. Phys.: Condens. Matter **11** (1999) 8933–8946. Printed in the UK PII: S0953-8984(99)03387-1

$Ag_{1-x}Na_xNbO_3$ (ANN) solid solutions: from disordered antiferroelectric $AgNbO_3$ to normal antiferroelectric $NaNbO_3$

A Kania and J Kwapuliński

Institute of Physics, University of Silesia, ul. Uniwersytecka 4, 40-007 Katowice, Poland

E-mail: kania@us.edu.pl

Received 13 April 1999, in final form 27 August 1999

Abstract. The ceramics of new solid solutions of $Ag_{1-x}Na_xNbO_3$ (ANN) have been sintered for the whole concentration range. Low frequency dielectric investigations (120–800 K) and DTA investigations (290–600 K) revealed a series of phase transitions. Two predominant aspects of the Na substitution have been found. The first one is related to a large increase of thermal hysteresis of the M_3–O_1 phase transition which points to its martensitic nature. The second one is related to the gradual disappearance of two diffuse $\varepsilon(T)$ maxima, associated with M_1–M_2 and M_2–M_3 phase transitions. The evolution from disordered antiferroelectric $AgNbO_3$ to normal antiferroelectric $NaNbO_3$ is considered. The influence of the oxygen octahedron size on the Nb ion dynamics is discussed. From the results obtained a phase diagram of the ANN system has been proposed.

1. Introduction

Low frequency, microwave and submillimetre dielectric studies of the silver niobate–tantalate solid solution $AgNb_{1-x}Ta_xO_3$ (ATN) showed that in this system, for non-ferroelectric phases, there is negligible dielectric dispersion for a very broad frequency range from 1 kHz up to approximately 100 GHz [1–4]. Moreover, a dispersion observed in the submillimetre region is solely related to one relaxational mode [2, 3]. The strength, relaxational frequency and temperature of its appearance depend strongly on the Nb/Ta ratio. In Raman scattering experiments this relaxational mode was observed as a strong central peak and showed very similar temperature and Nb/Ta concentration behaviour [5, 6]. The contribution of this relaxational mode to dielectric susceptibility [6, 7] explains the temperature dependences of the low frequency dielectric permittivity. It is also fully responsible for the appearance of the broad maximum of $\varepsilon(T)$ functions [8]. From the application point of view, especially the composition exhibiting this broad and flat maximum at room temperature should be considered since it has the smallest dielectric permittivity temperature coefficient. The ceramics of composition $AgTa_{0.57}Nb_{0.43}O_3$ fulfil this requirement. Experiments performed in the 1 GHz region [4] pointed to its high value of dielectric permittivity (375), the lack of dispersion, small temperature coefficient of the resonance frequency ($\Delta f/f_0 = 0$–0.022 in the temperature range -40–$60\,^\circ$C) and high quality factor Q (500). These results allow us to believe that the ATN system is very interesting and promising as a base for microwave and radio frequency materials [4, 9].

Both basic and application interests mentioned above are related to the appearance of the relaxational vibrations in a wide temperature range and their contribution to the dielectric response of the ATN system. This phenomenon is most significantly seen in pure silver niobate

0953-8984/99/458933+14$30.00

$AgNbO_3$ (AN) and appears in the background of the phase transition sequence. X-ray [10], electron diffraction [11], DTA, dielectric and domain structure studies [1, 8] showed that in silver niobate ceramics the following phase transitions are observed:

340 K—from the orthorhombic M_1 to the orthorhombic M_2,
540 K—from the orthorhombic M_2 to the orthorhombic M_3,
626 K—from the orthorhombic M_3 to the orthorhombic O_1,
634 K—from the orthorhombic O_1 to the orthorhombic O_2,
660 K—from the orthorhombic O_2 to the tetragonal T,
852 K—from the tetragonal T to the cubic C,

where M_1, M_2 and M_3 denote the phases with orthorhombic symmetry in rhombic orientation while O_1 and O_2 the phases with orthorhombic symmetry in parallel orientation. It was established that phase M_1 is ferroelectric, phases M_2 and M_3 are believed to be antiferroelectric and phases O_1, O_2, T and C are paraelectric [9–11]. It is worth recalling that the high temperature phase transitions (M_3–O_1, O_1–O_2, O_2–T and T–C) are detectable by the x-ray, DTA, dielectric and domain structure investigations. Whereas the low temperature phase transitions (M_1–M_2 and M_2–M_3) are observed only as diffused maxima of $\varepsilon(T)$ function and cannot be detected by x-ray [12], DTA or domain structure investigations and therefore they cannot be treated as transformations in terms of previous high temperature phase transitions. Taking these facts into account, it can be assumed that the AN as well as the ATN system are characterized by a coexistence of two subsystems. The first one—a strongly correlated system—leads to normal sharp phase transitions. The second one—probably associated with the disorder of Nb ion displacements—gives diffuse $\varepsilon(T)$ maxima and indicates the presence of a disordered antiferroelectric state [1, 4]. Disorder in silver niobate has already been found above 500 K by electron diffraction studies [11].

The microscopic origin of the relaxational mode that appears in the ATN system is not fully explained yet. The Raman [6, 13] and dielectric [2, 3] investigations pointed out the predominant role of the Nb ion dynamics in this phenomenon. This is due to the fact that with the increase in Ta content the temperature range of its appearance shifts towards lower temperatures and its contribution to the dielectric and Raman responses diminishes and finally disappears for pure silver tantalate $AgTaO_3$. However, the role of the Ag and O ions should not be neglected here as this phenomenon is unique among simple oxygen perovskites. Hence, it seems of interest to study the effect of Na substitution in the Ag sublattice on the properties of AN and therefore the main aim of this work is sintering and investigations of dielectric properties of the silver niobate–sodium niobate solid solutions $Ag_{1-x}Na_xNbO_3$ (ANN).

Sodium niobate $NaNbO_3$ (NN), which is isostructural to AN, exhibits a similar sequence of phase transitions [14, 15] but unlike AN is characterized by normal antiferroelectric behaviour. According to papers [14, 15], the following phase transitions are observed in $NaNbO_3$:

223 K—from the rhombohedral N to the orthorhombic P,
646 K—from the orthorhombic P to the orthorhombic R,
753 K—from the orthorhombic R to the orthorhombic S,
793 K—from the orthorhombic S to the orthorhombic T_1,
848 K—from the orthorhombic T_1 to the tetragonal T_2,
914 K—from the tetragonal T_2 to the cubic C,

where P denotes the phase with the orthorhombic symmetry in rhombic orientation while R, S and T_1 denote the phases with orthorhombic symmetry in parallel orientation. Phase N is ferroelectric, phases P and R are antiferroelectric whereas phases S, T_1 and T_2 are paraelectric [16–18]. All phase transitions in sodium niobate are observed as normal, sharp

ones. In some NN crystals the ferroelectric phase Q with orthorhombic symmetry was found at room temperature [16].

2. Sample preparation and x-ray tests

The $Ag_{1-x}Na_xNbO_3$ ceramics have been sintered by a solid state reaction. For all sintering processes the samples were placed in double corundum crucibles in which oxygen atmosphere was maintained. Ag_2O (99.5%), Na_2CO_3 (99.8%) and Nb_2O_5 (99.99%) were used as starting reagents. In the first stage pure AN and NN were sintered. The starting chemicals were weighed in equal molar quantities, mixed thoroughly, pressed into pellets and sintered for 3 hours at temperatures T_I equal to 1123 K and 1073 K for AN and NN, respectively. The obtained, prereacted materials were crushed, milled and mixed in required proportion. The pressed pellets were sintered at temperature T_{II} (1353–1473 K) for 2 hours and then again milled, pressed and finally sintered at temperature T_{III} (1393–1513 K) for 2.5 hours. The temperature of the second T_{II} and third T_{III} sintering processes increased linearly with the rise in Na concentration. Ceramics of good quality, light yellow in colour and 90–92% of the theoretical density were obtained. However, small amounts of metallic silver precipitations were detected for ceramics with a composition close to pure silver niobate.

X-ray powder studies were performed at room temperature with a modified DRON-1.5 x-ray diffractometer. The diffraction patterns contain the lines characteristic for a single phase of perovskite structure only. At room temperature all ANN ceramics exhibit the same orthorhombic symmetry as for both initial components. The evolution of the {220} and {321} diffraction lines as a function of the Na concentration is shown in figure 1. The shift of Bragg lines and the lack of their broadening indicate that sintered ANN samples are characterized by a homogeneous single phase state. The pseudoperovskite unit cell parameters $a_p = c_p$, b_p and monoclinic angle β as a function of the composition are plotted in figure 2. Lattice parameters decrease linearly while the monoclinic angle increases with increasing Na

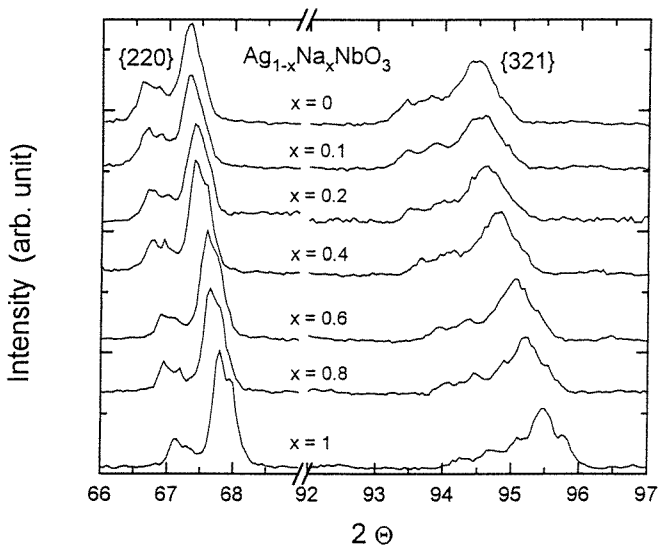

Figure 1. The {220} and {321} multiplets (Cu Kα_1 + Cu Kα_2) as a function of the Na concentration for $Ag_{1-x}Na_xNbO_3$ ceramics.

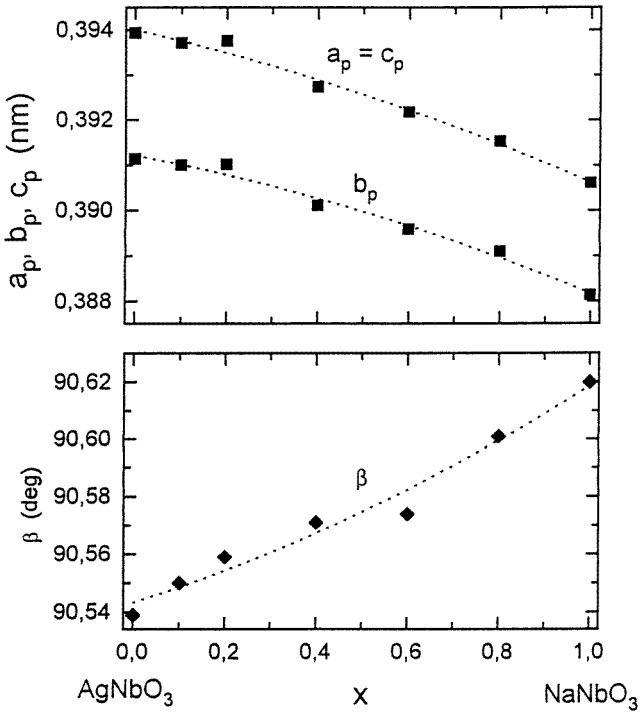

Figure 2. The lattice parameters of a pseudoperovskite unit cell of $Ag_{1-x}Na_xNbO_3$ solid solution.

concentration. The x-ray tests performed showed that solid solutions of the ANN ceramics are formed throughout the whole concentration range.

3. Dielectric investigations

Dielectric measurements were carried out for silver electroded samples using a BM595 *RLC* meter within the temperature range 120–900 K. The high temperature (573–900 K) ones were performed in air while the low temperature (120–573 K) ones in helium. The heating and cooling rate was 3 K min^{-1}. To avoid the influence of water contamination near 273 K (0 °C) the samples were kept in vacuum for 2 hours at about 520 K and then the cryostat was filled with helium. Prior to dielectric studies the samples were annealed in air for 0.5 hours at 920 K.

In general, all measured samples do not exhibit any significant dielectric dispersion for frequencies used, 200 Hz–20 kHz. Very small dispersion is observed only in the ferroelectric M_1 phase. At high temperature (above 600 K) a significant rise in dielectric permittivity with decrease of measuring frequency was observed. This effect is related to the increase of electric conductivity and cannot be treated as real dielectric dispersion. Therefore figures 1–6 present temperature dependences of dielectric permittivity and losses for a chosen frequency of 2 kHz and for the measuring electric field strength of 20 V cm^{-1}.

3.1. Dielectric properties of $AgNbO_3$

Figure 3 presents the temperature dependences of dielectric permittivity for $AgNbO_3$. They are typical for silver niobate and exhibit characteristic anomalies. On heating, after an initial

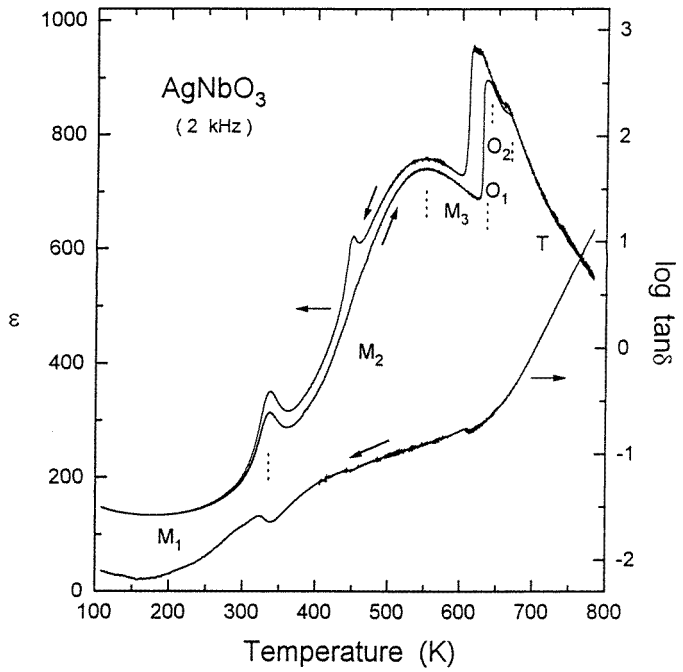

Figure 3. Temperature dependences of dielectric permittivity and losses for $AgNbO_3$ ceramics.

slight decrease, the dielectric permittivity increases with rise in temperature and two broad local maxima at 340 K and 540 K are observed. They correspond to M_1–M_2 and M_2–M_3 phase transitions, respectively. A sharp jump of the $\varepsilon(T)$ function at 626 K is associated with the antiferroelectric–paraelectric (M_3–O_1) phase transition. Above this point, dielectric permittivity drops with temperature increase. On the decreasing part of the $\varepsilon(T)$ dependence two small anomalies are visible at 634 K (O_1–O_2) and 660 K (O_2–T). The M_3–O_1, O_1–O_2 and O_2–T phase transitions are accompanied by a thermal hysteresis of several degrees, whereas the thermal hysteresis of the M_1–M_2 and M_2–M_3 phase transitions is unnoticeable. The temperature dependence of dielectric losses $\tan\delta(T)$ exhibits two local maxima associated with the appearance of ferroelectric and antiferroelectric phases. An additional local maximum of $\varepsilon(T)$ is observed (only on cooling) near 440 K. This anomaly cannot be connected with any phase transition and its origin at present is unknown.

3.2. Dielectric properties of $NaNbO_3$

Figure 4 presents the temperature dependences of dielectric permittivity for $NaNbO_3$. On heating, $\varepsilon(T)$ evolves as follows. The dielectric permittivity is nearly stable within the temperature range 100–400 K. Then it increases when the temperature approaches the P–R phase transition (668 K) and after a jump of the $\varepsilon(T)$ function it decreases. The small anomaly near 800 K, which is seen as a deflection point of the $\varepsilon(T)$ curve, indicates the S–T_1 phase transition. The biggest differences between the heating and cooling processes are connected with the main P–R phase transition. The high value of the detected thermal hysteresis ($\sim$70 K) is typical for the NN ceramics and much larger than the one observed for single crystals [19]. The P–R phase transition is accompanied by a local maximum of temperature dependence of dielectric losses $\tan\delta(T)$.

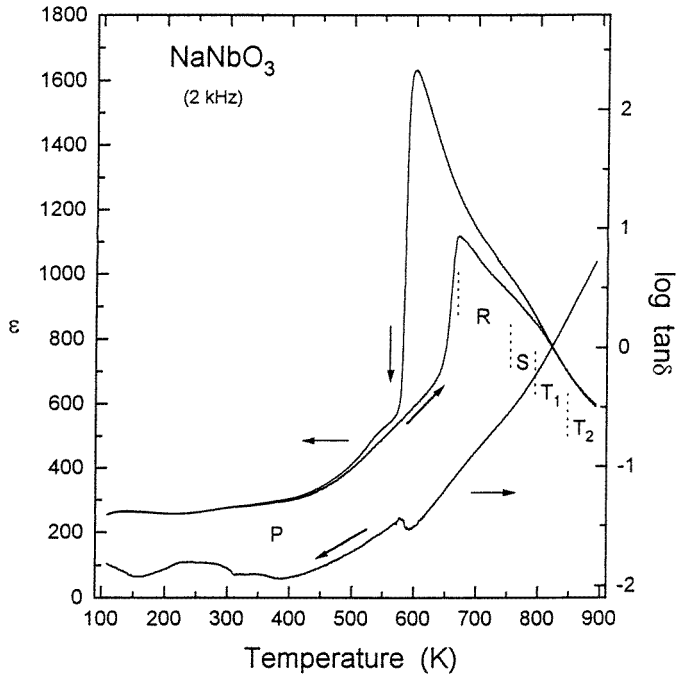

Figure 4. Temperature dependences of dielectric permittivity and losses for $NaNbO_3$ ceramics.

Furthermore, in the background of this typical NN behaviour, a small bump of $\varepsilon(T)$ dependence near 540 K is clearly seen. This proves that when relaxational processes are present in NN then their contribution to dielectric response is not so important as in the case of AN. This anomaly may also point to the presence of traces of the Q phase in the measured ceramics. The coexistence of P and Q phases at room temperature has been found for some NN samples [17, 20, 21].

3.3. Dielectric properties of $Ag_{1-x}Na_xNbO_3$

The temperature dependences of dielectric permittivity for $Ag_{0.8}Na_{0.2}NbO_3$ and $Ag_{0.4}Na_{0.6}NbO_3$ are shown in figures 5 and 6, respectively. They show gradual evolution of dielectric properties from one characteristic border case to the other. This evolution is described below in comparison with silver niobate. Three main features related to the M_3–O_1, M_2–M_3 and M_1–M_2 phase transition can be distinguished. With the increase of Na concentration:

(i) The thermal hysteresis of the M_3–O_1 phase transition increases from 20 K for AN to about 90 K for $x = 0.6$ and then decreases to 70 K in the case of NN. On heating, the temperature of this phase transition increases from 626 K ($x = 0$) to the maximum value of 720 K ($x = 0.6$) and then decreases to 668 K ($x = 1$). On cooling, similar shifts of the phase transition temperature versus Na concentration are observed but they are much smaller in magnitude. As a result, the described influence of the Na substitution on the thermal hysteresis of the M_3–O_1 phase transition is observed. Moreover, for samples with $0 \leqslant x \leqslant 0.6$, for which the significant increase of transition temperature on heating takes place, the jump of the dielectric permittivity associated with the phase transition first decreases and then for $x > 0.6$ increases. On cooling, when no significant shifts of the

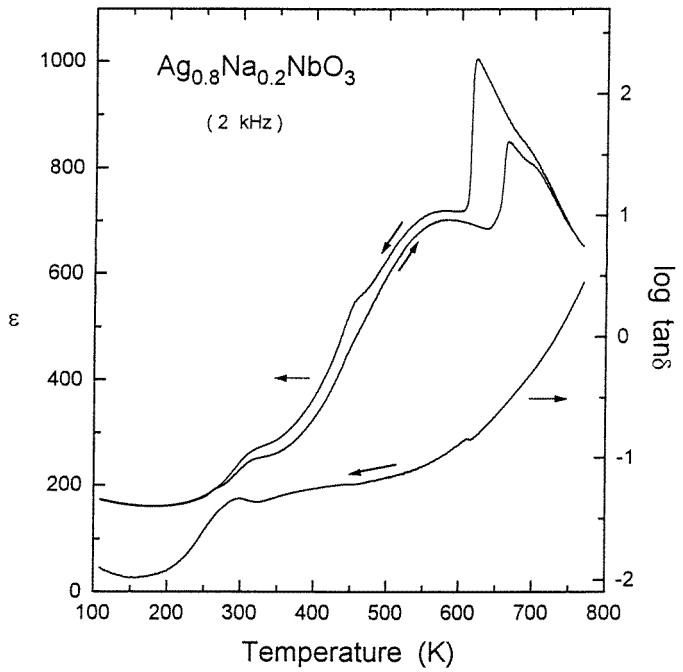

Figure 5. Temperature dependences of dielectric permittivity and losses for $Ag_{0.8}Na_{0.2}NbO_3$ ceramics.

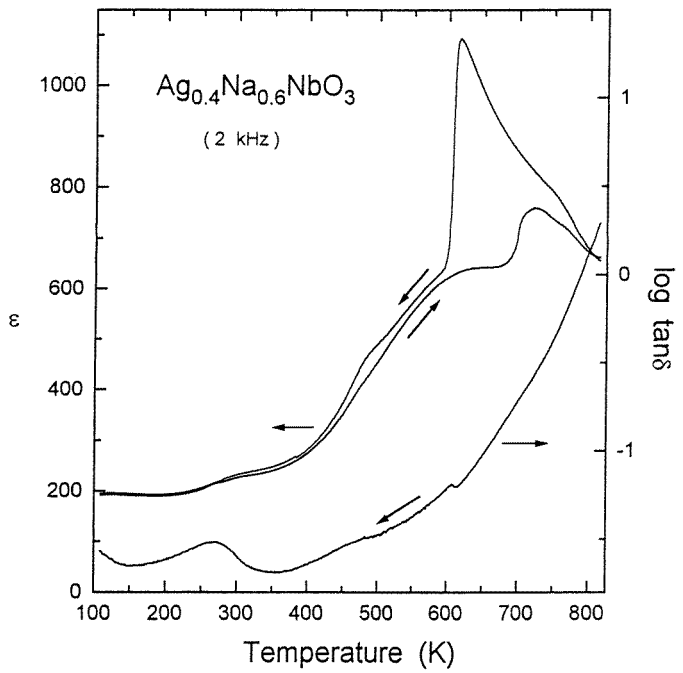

Figure 6. Temperature dependences of dielectric permittivity and losses for $Ag_{0.4}Na_{0.6}NbO_3$ ceramics.

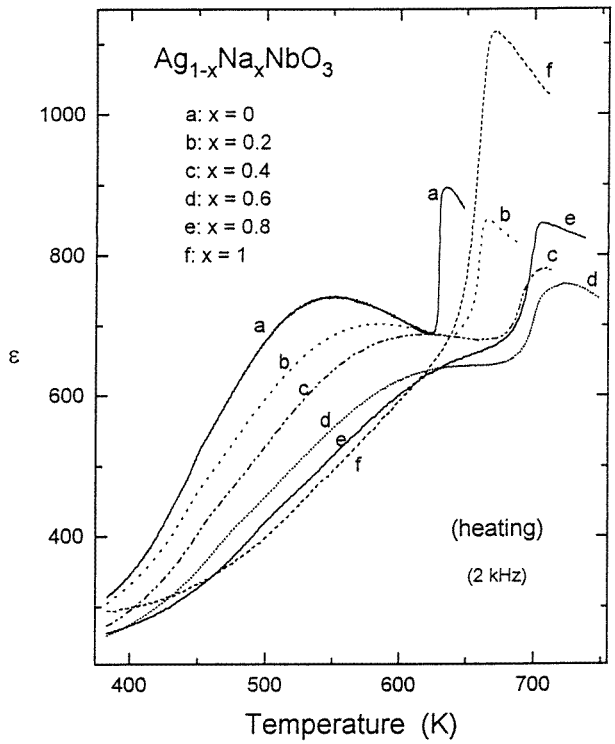

Figure 7. Dielectric permittivity of $Ag_{1-x}Na_xNbO_3$ solid solution as a function of temperature and composition in the vicinity of the M_2–M_3 and M_3–O_1 phase transitions (on heating).

phase transition temperature occur, the associated jump of $\varepsilon(T)$ increases linearly with the rise in Na concentration. Above this phase transition temperature both on cooling and on heating the replacement of the Ag ions by the Na ones causes an increase of the dielectric permittivity. The evolution of dielectric properties of the ANN solid solutions in the vicinity of the M_3–O_1 and M_2–M_3 phase transitions is clearly seen in figure 7 and figure 8.

(ii) The broad maximum of $\varepsilon(T)$ near 550 K related to the M_2–M_3 phase transition gradually decreases, becomes much broader and shifts towards higher temperatures. For pure sodium niobate only a small hump of $\varepsilon(T)$ in this temperature region is noticeable. The evolution of this phase transition is much more visible on heating (figure 7) than on cooling (figure 8) due to the large thermal hysteresis described above of the M_3–O_1 phase transition.

(iii) The local maximum of $\varepsilon(T)$ near 340 K related to M_1–M_2 phase transition decreases and shifts towards lower temperatures (figure 9). The anomaly of temperature dependence of losses $\tan\delta(T)$ does not disappear quickly and even for NN a small local maximum is seen (figures 3–6).

4. DTA investigations

DTA investigations were performed using UNIPAN DSC 605 equipment. Experiments were carried out for crushed ANN ceramics in the temperature range 300–720 K on heating and

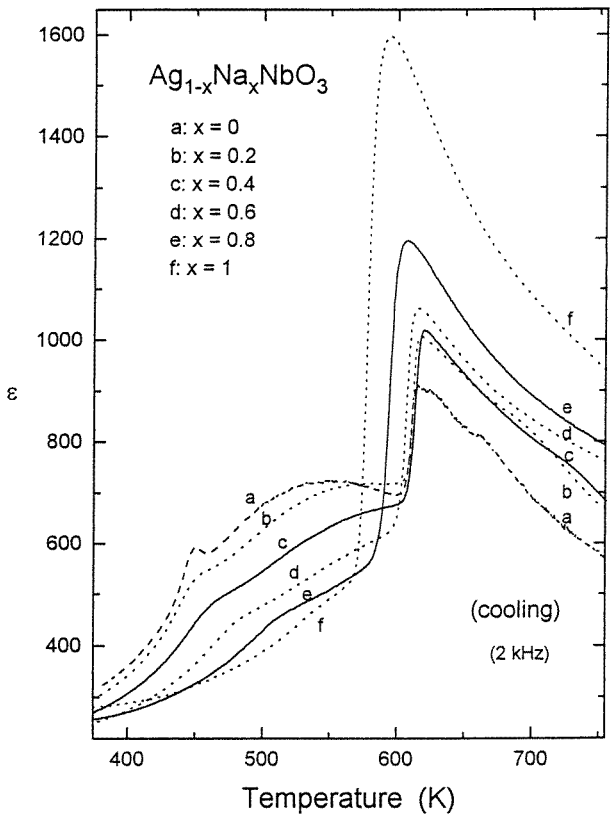

Figure 8. Dielectric permittivity of $Ag_{1-x}Na_xNbO_3$ as a function of temperature and composition in the vicinity of the M_2–M_3 and M_3–O_1 phase transitions (on cooling).

cooling at a rate of 3 K min^{-1}. Within this temperature range the DTA curves showed an anomaly connected with M_3–O_1 or P–R phase transition only (when referred to AN or NN, respectively) and they are shown in figure 10. Temperatures T_p and latent heats Q_p determined from the DTA peaks versus the ANN composition are plotted in figure 11. They show that with the rise in Na concentration:

(i) on heating, the temperature T_p of the endothermic peak initially increases from 629 K ($x = 0$) to 704 K ($x = 0.6$) and then decreases to 648 K while the associated latent heat Q_p first decreases from 0.30 kJ mol^{-1} ($x = 0$) to 0.07 kJ mol^{-1} ($x = 0.6$) and then increases to 0.15 kJ mol^{-1} ($x = 1$),

(ii) on cooling, the temperature T_p of the exothermic peak slowly increases from 607 K ($x = 0$) to 628 K ($x = 0.6$) and then decreases to 605 K ($x = 1$) while latent heat Q_p slightly decreases from 0.32 kJ mol^{-1} ($x = 0$) to about 0.22 kJ mol^{-1} ($x = 1$),

(iii) the thermal hysteresis of this phase transition increases from 22 K ($x = 0$) to 76 K ($x = 0.6$) and then decreases to 43 K ($x = 1$).

The DTA results confirmed that the influence of Na substitution on the M_3–O phase transition is the same as in the case of dielectric measurements.

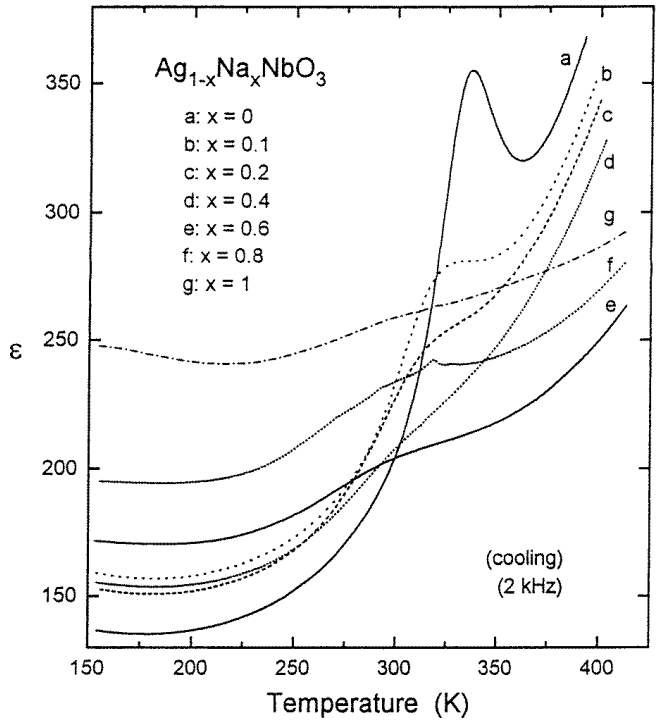

Figure 9. Dielectric permittivity of $Ag_{1-x}Na_xNbO_3$ as a function of temperature and composition in the vicinity of the M_1–M_2 phase transition (on cooling).

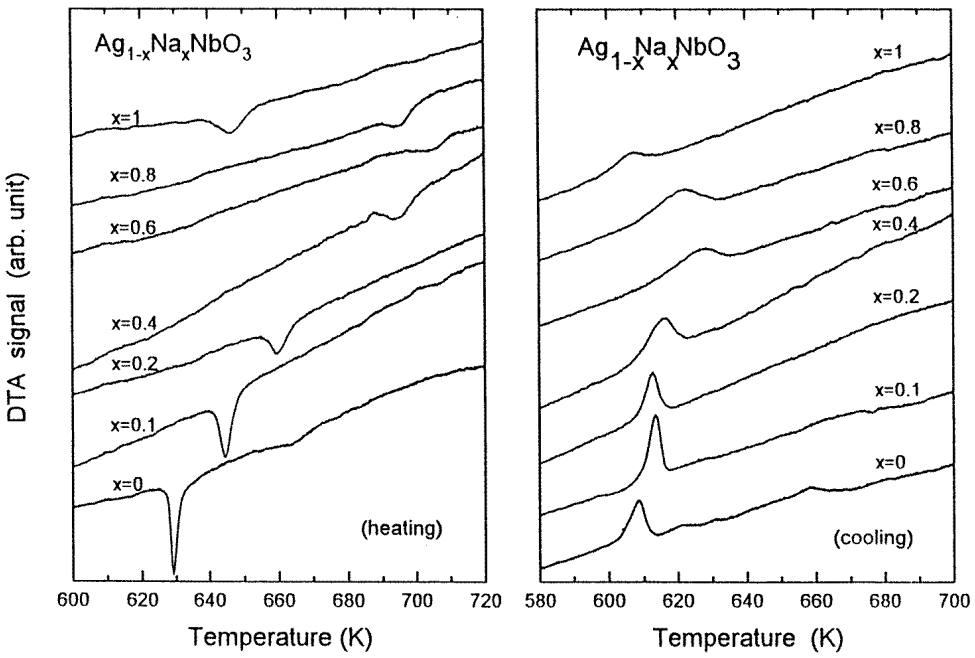

(a) (b)

Figure 10. DTA curves on heating (a) and cooling (b) for $Ag_{1-x}Na_xNbO_3$ solid solutions.

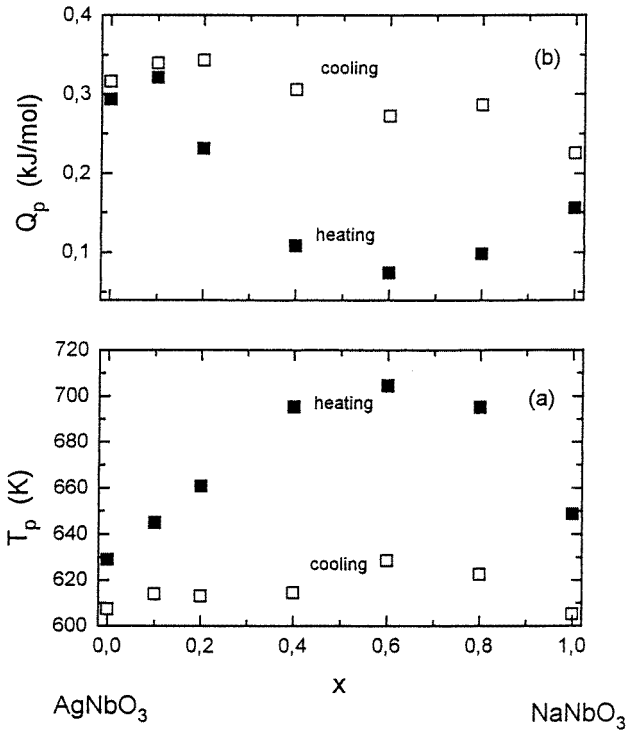

Figure 11. Temperatures T_p (a) and latent heats Q_p (b) determined from DTA experiments versus $Ag_{1-x}Na_xNbO_3$ composition.

5. Summary and discussion

The technology described made it possible to obtain ceramics of a new $AgNbO_3$–$NaNbO_3$ solid solution system. The use of oxygen atmosphere during sintering, as in the earlier ATN technology [8, 9], gave ceramics of good quality, though small quantities of silver metallic precipitation's were noticed. X-ray tests showed that the obtained ANN ceramics consist of a single perovskite phase and at room temperature exhibit the orthorhombic symmetry for the whole concentration range. The lattice parameters $a_p = c_p$ and b_p of the pseudoperovskite cell decrease and the monoclinic angle β increases with the increase in Na concentration (figure 2). This indicates that size and volume of oxygen octahedra decrease with the rise in Na concentration. This in turn limits the degree of freedom of the Nb ion displacement from the oxygen octahedron centre.

The low frequency dielectric investigations have not shown any significant dielectric dispersion for studied ANN ceramics. Temperatures of particular phase transitions (on heating) determined from local maxima of $\varepsilon(T)$ dependences and the DTA anomalies are plotted versus ANN composition in figure 12. The high temperature (above 800 K) phase transitions related to the oxygen octahedron tiltings are not included as they are not detectable in dielectric investigations and occur at temperatures higher than our DTA equipment limit. The obtained phase diagram does not show essential changes of symmetry and of phase transition temperatures. Such a behaviour was expected since the ANN system consists of two isostructural compounds exhibiting a similar sequence of structural phase transitions and a similar type of electric ordering. Nevertheless, a strong influence of Na substitution on

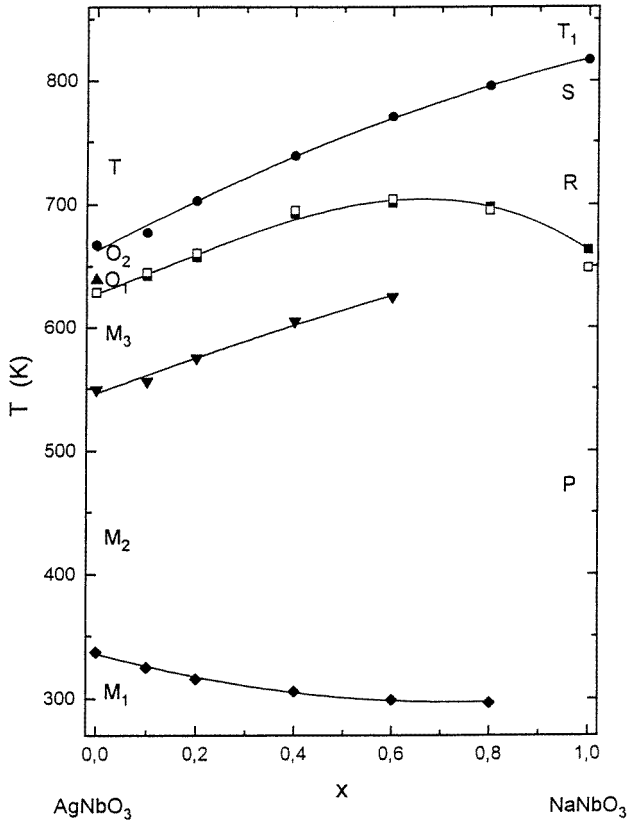

Figure 12. Phase diagram of $Ag_{1-x}Na_xNbO_3$ solid solutions (on heating). Empty symbols denote phase transition temperatures determined from the DTA results. Solid symbols denote phase transition temperatures determined from dielectric results. The symmetry of $AgNbO_3$ and $NaNbO_3$ is indicated.

the nature of phase transitions is manifested. As can be clearly seen (figures 7–9), the Na substitution affects the structural phase transition M_3–O_1 in a different way than M_1–M_2 and M_2–M_3 which are not purely structural.

The sodium substitution markedly increases the thermal hysteresis of the main antiferroelectric phase transition denoted as M_3–O_1. In order to explain this feature we adopted the concept of martensitic phase transition which was proposed for the P–R phase transition in sodium niobate [19, 22]. For martensitic phase transitions a large shift of the phase transition temperature due to internal and external stresses is observed [23]. Therefore, even a small inhomogeneity of the ion distribution which is expected in solid solutions and other lattice imperfections may cause significant internal stresses. One can expect that this inhomogeneity and the resulting internal stress should maximize for $x = 0.5$ and that was the case in our studies. The P–R phase transition in NN is characterized by a large thermal hysteresis: 40–70 K for ceramics ([19] and this paper) and 35 K for single crystals [24].

The influence of Na substitution on the behaviour of the M_1–M_2 and M_2–M_3 phase transitions is much more distinct. Two maxima of $\varepsilon(T)$ functions related to these phase transitions gradually decrease with rise in Na concentration and almost disappear for pure NN. The temperature of M_1–M_2 phase transitions shifts towards lower

temperatures (≈ -1 K %$^{-1}$ mol^{-1}) while in the case of M_2–M_3 towards higher temperatures ($\approx +2$ K %$^{-1}$ mol^{-1}).

It is noteworthy that all accessible literature data show exactly the same diffused maxima of the $\varepsilon(T)$ function near the M_2–M_3 phase transition, regardless of the quality of silver niobate investigated. Therefore, this specific behaviour may be considered as an intrinsic property of silver niobate. Earlier Raman [6, 13] and submillimetre dielectric investigations [2, 3] of the ATN system made it possible to link the appearance of the submillimetre relaxational mode with the low frequency dielectric response and pointed to the predominant role of Nb ion dynamics in this phenomenon. These results allowed us to propose the presence of disorder in the Nb ion displacements. Consequently, the diffuse M_2–M_3 phase transition is associated with the disordered antiferroelectric state in the ATN system [1, 4]. The Raman experiments performed for the ANN solid solutions considered here showed a very similar (to ATN) temperature correlation between the appearance of the central component in the Raman spectra and the diffuse maximum of low frequency dielectric permittivity [25]. Thus, an attempt to find a link between low and high frequency phenomena seems feasible. In spite of the fact that low frequency dielectric results make it impossible to find the microscopic origin of this phenomenon, some general conclusions based on a simple geometrical approach [26, 27] can be drawn.

Geometrical considerations showed that silver niobate $AgNbO_3$ with its ionic radius relations is placed near the border between the oxygen perovskites with a displacive type of phase transition and those of the tilting octahedron type [26]. In the series of Na, Ag and K niobates, the silver niobate with the average size of pseudocubic unit cell at room temperature equal to 0.3934 nm is located between antiferroelectric sodium niobate (0.3909 nm) (for which the tilting octahedra is the predominant mechanism of the phase transitions) and displacive-type ferroelectric potassium niobate (0.4014 nm) [28]. The parallel and antiparallel Nb ion displacements from the oxygen octahedra centre lead to ferro- and antiferroelectric states in $KNbO_3$ and $NaNbO_3$, respectively. In silver niobate the Nb ions possess an intermediate freedom of movement and thus some competition between both mentioned types of displacement ought to be expected. This may be the reason for the appearance of the relaxational mode. As a result, some disorder within the antiferroelectric state occurs. At low temperature this state transforms into the weak ferroelectric M_1 phase ($P_s = 0.04$ μC cm^{-2}) [29]. Hence we may conclude that the M_1, M_2 and M_3 phases are characterized by different states of the Nb sublattice even though there is no pure structural transformation between them.

The Na substitution causes a decrease of the oxygen octahedron size and diminishes the freedom of Nb ions causing a gradual decrease of the M_2–M_3 phenomenon. The assumption that transformation from the disordered (AN) to the ordered antiferroelectric (NN) takes place in the ANN system can be stated though in some papers a disorder in sodium niobate was found [30, 31]. In addition, the specific M_2–M_3 behaviour of the silver niobate based materials can be associated with the oxygen octahedron size effect. Moreover, dielectric studies of $Ag_{1-x}K_xNbO_3$ solid solutions [32] showed that small addition of bigger potassium ions (5% mol) leads to the disappearance of the described M_2–M_3 phenomenon which supports our simple geometrical approach.

The TEM studies showed a disorder in silver niobate above 500 K [11]. The authors attribute it to the oxygen sublattice. These two types of disorder, namely the disorder in the Nb ion displacements and the disorder in the oxygen octahedron tilting scheme, should not exclude each other. Hence it seems understandable that at room temperature (M_1 phase) both the TEM [33] and the x-ray studies [34] revealed a certain modulation of the perovskite structure of silver niobate.

Acknowledgments

The authors would like to thank Dr A Molak, Professor J Hañderek, Professor K Roleder, Professor J Petzelt, Professor G Kugel and Professor M Hafid for helpful discussions.

References

[1] Kania A 1998 *Ferroelectrics* **205** 19
[2] Volkov A A, Gorshunov B P, Komandin G, Fortin W, Kugel G E, Kania A and Grigas J 1995 *J. Phys.: Condens. Matter* **7** 785
[3] Petzelt J, Kamba S, Kozlov G V and Volkov A A 1996 *Ferroelectrics* **176** 145
[4] Petzelt J *et al* 1999 *Ferroelectrics* **223** 235
[5] Kania A, Roleder K, Kugel G E and Fontana M D 1986 *J. Phys. C: Solid State Phys.* **19** 9
[6] Hafid M, Kugel G E, Kania A, Roleder K and Fontana M D 1992 *J. Phys.: Condens. Matter* **4** 2333
[7] Fortin W, Kugel G E, Grigas J and Kania A 1996 *J. Appl. Phys.* **79** 4273
[8] Kania A 1983 *Phase Transitions* **3** 131
[9] Valant M and Suvorov D 1999 *J. Am. Ceram. Soc.* **82** 88
[10] Pawełczyk M 1987 *Phase Transitions* **8** 273
[11] Verweft M, Van Dyck D, Brabers V A M, Van Landuyt J and Amelinckx S 1989 *Phys. Status Solidi* a **112** 451
[12] Miga S and Dec J 1999 *J. Appl. Phys.* **85** 1756
[13] Kania A, Hafid M, Kugel G E, Fontana M D and Roleder K 1988 *Ferroelectrics* **80** 141
[14] Glazer A M and Megaw H 1973 *Acta Crystallogr.* A **29** 489
[15] Megaw H 1974 *Ferroelectrics* **7** 87
[16] Lefkowitz L, Łukaszewicz K and Megaw H D 1966 *Acta Crystallogr.* **20** 670
[17] Sakowski-Cowley C A, Łukaszewicz K and Megaw H D 1969 *Acta Crystallogr.* B **25** 851
[18] Avogadro A, Bonera G, Borsa F and Rigamonti A 1974 *Phys. Rev.* B **9** 3905
[19] Molak A 1997 *J. Phys.: Condens. Matter* **9** 1263
[20] Darlington C N W 1971 *Ferroelectrics* **3** 9
[21] Molak A, Onodera A and Pawełczyk M 1995 *Ferroelectrics* **172** 295
[22] Dec J and Kwapuliński J 1989 *Phase Transitions* **18** 1
[23] Kartha S 1995 *Phys. Rev.* B **52** 803
[24] Cross L E and Nicholson B J 1955 *Phil. Mag.* **46** 453
[25] Hafid M, Kania A and Kugel E G in preparation
[26] Cassan-Ogly F A and Naish V E 1986 *Acta Crystallogr.* B **42** 307
[27] Thomas N W 1989 *Acta Crystallogr.* B **45** 337
[28] Galasso F 1969 *Structure, Properties and Preparation of Perovskite Type Compounds* (Oxford: Pergamon)
[29] Kania A and Roleder K 1984 *Ferroelectr. Lett.* **2** 51
[30] Chen J and Peng D 1988 *Phys. Status Solidi* a **109** 171
[31] Denoyer F, Comes R, Lambert M and Gunter A 1974 *Acta Crystallogr.* A **30** 423
[32] Łukaszewski M 1983 *Ferroelectr. Lett.* **44** 323
[33] Verwerft M, van Tendeloo G, van Landuyt J, Coene W and Amelinckx S 1988 *Phys. Status Solidi* a **109** 67
[34] Fabry J, Zikmund Z, Kania A and Petricek V *Acta Crystallogr.* submitted